Analytical Calculation of Waves in a Muffin–Tin Structure

M. Filtz
Technische Universität Berlin, EN-2, Einsteinufer 17, D-10587 Berlin

Abstract

For acceleration at very high frequencies planar RF structures have been proposed elsewhere. In the present paper an analytical solution for the fields in a muffin–tin structure is given using the mode matching technique. The resulting em–field is splitted in transverse electric as well as transverse magnetic components w.r.t. the matching plane, i.e. the transition plane from the drift region to the cavities. Diagrams are presented showing the fields of the first accelerating and deflecting modes. Furthermore the longitudinal shunt impedance divided by the Q–value is computed.

1 INTRODUCTION

The present paper treats analytically a periodic planar structure as shown in Fig.1. In [1] numerical results are

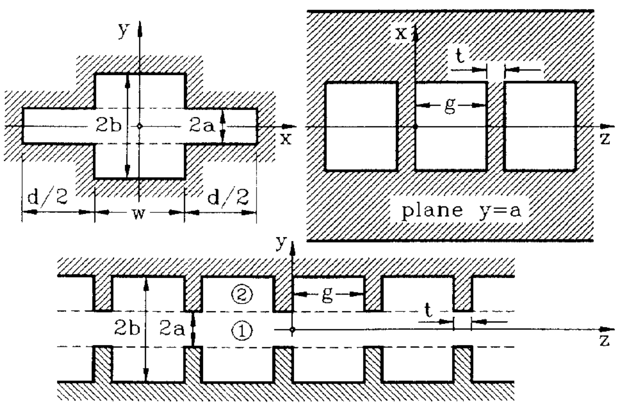

Figure 1: geometry of the structure under consideration for three points of view

presented for the basic RF parameters calculated with MAFIA. But the geometry of this structure allows also an analytical solution. The method used in this paper is field matching. The advantage over a purely numerical method is, that we can in principle extend the length of the side openings to infinity. In this case the discrete set of modes has to be replaced by a continuous spectrum. But within the scope of this work electric walls at $x = \pm(w+d)/2$ are assumed.

There are various possibilities to solve the given problem using orthogonal expansions. They essentially differ in choosing the matching plane. Referring to Fig.1 we separate the whole region into two sub–regions: region 1 called the drift region and region 2 called the cavity region. So the matching planes are $y = \pm a$.

Because of the necessary two–dimensional Fourier expansion the numerical evaluation will consume a lot of time and store. Therefore we make use of symmetry w.r.t. the planes $x = 0$ and $y = 0$ and consider 4 cases with boundary conditions defined in Fig.2. The resulting electromagnetic

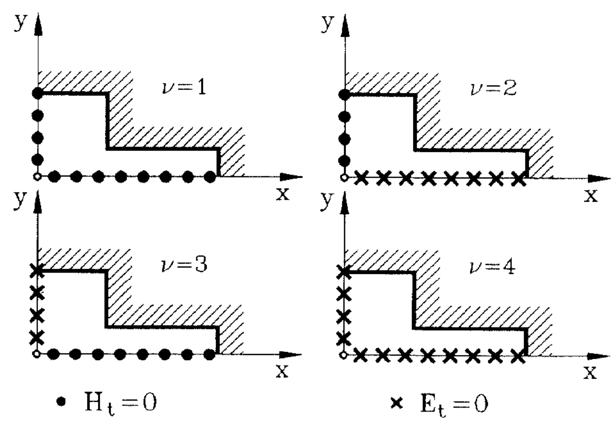

Figure 2: defining 4 problems with different boundary conditions

field is splitted in transverse electric (TE_y) and transverse magnetic (TM_y) components perpendicular to the plane $y = a$ in order to match the tangential field in an easy way using orthogonal vector functions.

2 FIELDS IN THE DIFFERENT REGIONS

By reason of the infinite periodic structure the Floquet theorem permits the decomposition of the fields in region 1 in space harmonics with the phase constants

$$\beta_n = \beta_0 + 2\pi n/(g+t)\ ,\ n = 0, 1, 2, \ldots$$

where $\beta_0(g+t)$ is a given phase advance per cell. In region 2 instead of space harmonics we have to choose standing wave functions. So we can write the tangential fields (w.r.t. $y = a$) in the following compact matrix notation

$$\vec{E}^{(\nu)}_{1,t} = Z_0 \vec{\mathbf{F}}^{(\nu)T}(x,z)\left\{-\mathbf{V}^{(\nu)}_{+}(y) + (-)^{\nu}\mathbf{V}^{(\nu)}_{-}(y)\right\}\mathbf{A}^{(\nu)}$$

$$\vec{e}_y \times \vec{H}^{(\nu)}_{1,t} = \vec{\mathbf{F}}^{(\nu)T}(x,z)\mathbf{Y}^{(\nu)}_{1}\left\{\mathbf{V}^{(\nu)}_{+}(y) + (-)^{\nu}\mathbf{V}^{(\nu)}_{-}(y)\right\}\mathbf{A}^{(\nu)}$$

$$\vec{E}^{(\nu)}_{2,t} = Z_0 \vec{\mathbf{G}}^{(\nu)T}(x,z)\left\{-\mathbf{W}^{(\nu)}_{+}(y) + \mathbf{W}^{(\nu)}_{-}(y)\right\}\mathbf{B}^{(\nu)}$$

$$\vec{e}_y \times \vec{H}_{2,t}^{(\nu)} = \vec{\mathbf{G}}^{(\nu)T}(x,z)\mathbf{Y}_2^{(\nu)}\left\{\mathbf{W}_+^{(\nu)}(y) + \mathbf{W}_-^{(\nu)}(y)\right\}\mathbf{B}^{(\nu)}$$

$$\mathbf{V}_\pm^{(\nu)} = \exp\left(\mp \mathrm{j}\mathbf{K}_1^{(\nu)}y\right)\ ,\ \mathbf{W}_\pm^{(\nu)} = \exp\left(\mp \mathrm{j}\mathbf{K}_2^{(\nu)}[y-b]\right) \tag{1}$$

where $Z_0 = \sqrt{\frac{\mu_0}{\varepsilon_0}}$ and ν corresponds to the boundary conditions of Fig.2. The matrices in (1) have the following meaning:

- the column matrices

$$\begin{aligned}\vec{\mathbf{F}}^{(\nu)}(x,z) &= \vec{e}_x\mathbf{F}_x^{(\nu)}(x,z) + \vec{e}_z\mathbf{F}_z^{(\nu)}(x,z)\\ \vec{\mathbf{G}}^{(\nu)}(x,z) &= \vec{e}_x\mathbf{G}_x^{(\nu)}(x,z) + \vec{e}_z\mathbf{G}_z^{(\nu)}(x,z)\end{aligned} \tag{2}$$

contain the elements

$$F_{x,mn}^{(1),(2)} = \mathrm{e}^{-\mathrm{j}\beta_n z}\sin\frac{(2m-1)\pi x}{w+d}\begin{cases}\mathrm{j}\beta_n & (TE_y)\\ -\frac{(2m-1)\pi}{w+d} & (TM_y)\end{cases}$$

$$F_{z,mn}^{(1),(2)} = \mathrm{e}^{-\mathrm{j}\beta_n z}\cos\frac{(2m-1)\pi x}{w+d}\begin{cases}\frac{(2m-1)\pi}{w+d} & (TE_y)\\ -\mathrm{j}\beta_n & (TM_y)\end{cases}$$

$$G_{x,mn}^{(1),(2)} = \sin\frac{n\pi z}{g}\sin\frac{(2m-1)\pi x}{w}\begin{cases}\frac{n\pi}{g} & (TE_y)\\ -\frac{(2m-1)\pi}{w} & (TM_y)\end{cases}$$

$$G_{z,mn}^{(1),(2)} = \cos\frac{n\pi z}{g}\cos\frac{(2m-1)\pi x}{w}\begin{cases}\frac{(2m-1)\pi}{w} & (TE_y)\\ \frac{n\pi}{g} & (TM_y)\end{cases}$$

for $\nu = 1,2$ and

$$F_{x,mn}^{(3),(4)} = \mathrm{e}^{-\mathrm{j}\beta_n z}\cos\frac{2m\pi x}{w+d}\begin{cases}\mathrm{j}\beta_n & (TE_y)\\ \frac{2m\pi}{w+d} & (TM_y)\end{cases}$$

$$F_{z,mn}^{(3),(4)} = \mathrm{e}^{-\mathrm{j}\beta_n z}\sin\frac{2m\pi x}{w+d}\begin{cases}-\frac{2m\pi}{w+d} & (TE_y)\\ -\mathrm{j}\beta_n & (TM_y)\end{cases}$$

$$G_{x,mn}^{(3),(4)} = \sin\frac{n\pi z}{g}\cos\frac{2m\pi x}{w}\begin{cases}\frac{n\pi}{g} & (TE_y)\\ \frac{2m\pi}{w} & (TM_y)\end{cases}$$

$$G_{z,mn}^{(3),(4)} = \cos\frac{n\pi z}{g}\sin\frac{2m\pi x}{w}\begin{cases}-\frac{2m\pi}{w} & (TE_y)\\ \frac{n\pi}{g} & (TM_y)\end{cases}$$

for $\nu = 3,4$.

- the diagonal matrices $\mathbf{K}_1^{(\nu)}$, $\mathbf{K}_2^{(\nu)}$ and $\mathbf{Y}_1^{(\nu)}$, $\mathbf{Y}_2^{(\nu)}$ with modal wavenumbers and wave admittances respectively contain the elements

$$K_{1,mn}^{(1),(2)} = \sqrt{k^2 - \beta_n^2 - \left(\frac{(2m-1)\pi}{w+d}\right)^2}\ ,$$

$$K_{1,mn}^{(3),(4)} = \sqrt{k^2 - \beta_n^2 - \left(\frac{2m\pi}{w+d}\right)^2}\ ,$$

$$K_{2,mn}^{(1),(2)} = \sqrt{k^2 - \left(\frac{n\pi}{g}\right)^2 - \left(\frac{(2m-1)\pi}{w}\right)^2}$$

$$K_{2,mn}^{(3),(4)} = \sqrt{k^2 - \left(\frac{n\pi}{g}\right)^2 - \left(\frac{2m\pi}{w}\right)^2}$$

$$Y_{i,mn}^{(\nu)} = \begin{cases}K_{i,mn}^{(\nu)}/k & (TE_y)\\ k/K_{i,mn}^{(\nu)} & (TM_y)\end{cases}\ ,\ k = \frac{\omega}{c_0} \tag{3}$$

3 FIELD MATCHING

The characteristic coupling matrix for the transition from region 1 to region 2 reads

$$\int_0^g\int_0^{w/2}\vec{\mathbf{G}}^{(\nu)}(x,z)\,\overset{*}{\vec{\mathbf{F}}}{}^{(\nu)T}(x,z)\,\mathrm{d}x\,\mathrm{d}z = \mathbf{M}^{(\nu)} \tag{4}$$

and due to orthogonality the following integrals deliver diagonal matrices

$$\int_0^{g+t}\int_0^{(w+d)/2}\vec{\mathbf{F}}^{(\nu)}(x,z)\,\overset{*}{\vec{\mathbf{F}}}{}^{(\nu)T}(x,z)\,\mathrm{d}x\,\mathrm{d}z = \mathbf{I}^{(\nu)}$$

$$\int_0^g\int_0^{w/2}\vec{\mathbf{G}}^{(\nu)}(x,z)\vec{\mathbf{G}}^{(\nu)T}(x,z)\,\mathrm{d}x\,\mathrm{d}z = \mathbf{J}^{(\nu)} \tag{5}$$

where the asterisk (*) describes a conjugate complex number and the superscript (^{T}) the transpose of a matrix.

With the abbreviations

$$\tilde{\mathbf{V}}^{(\nu)} = \frac{\left[\mathbf{V}_-^{(\nu)}(a)\right]^2 + (-)^\nu\mathbf{1}}{\left[\mathbf{V}_-^{(\nu)}(a)\right]^2 - (-)^\nu\mathbf{1}}\ ,\ \tilde{\mathbf{W}}^{(\nu)} = \frac{\left[\mathbf{W}_+^{(\nu)}(a)\right]^2 - \mathbf{1}}{\left[\mathbf{W}_+^{(\nu)}(a)\right]^2 + \mathbf{1}}$$

$$\tilde{\mathbf{A}}^{(\nu)} = \mathbf{A}^{(\nu)}\left\{\mathbf{V}_+^{(\nu)}(a) - (-)^\nu\mathbf{V}_-^{(\nu)}(a)\right\}$$

$$\tilde{\mathbf{B}}^{(\nu)} = \mathbf{B}^{(\nu)}\left\{\mathbf{W}_+^{(\nu)}(a) + \mathbf{W}_-^{(\nu)}(a)\right\} \tag{6}$$

the continuity and boundary conditions in the plane $y = a$ finally yield the homogenous system of linear equations

$$\left\{\mathbf{Y}_2^{(\nu)}\mathbf{J}^{(\nu)} - \overset{*}{\mathbf{M}}{}^{(\nu)}\frac{\tilde{\mathbf{V}}^{(\nu)}\mathbf{Y}_1^{(\nu)}}{\mathbf{I}^{(\nu)}}\mathbf{M}^{(\nu)T}\tilde{\mathbf{W}}^{(\nu)}\right\}\tilde{\mathbf{B}}^{(\nu)} = 0$$

$$\mathbf{I}^{(\nu)}\tilde{\mathbf{A}}^{(\nu)} = \mathbf{M}^{(\nu)T}\tilde{\mathbf{W}}^{(\nu)}\tilde{\mathbf{B}}^{(\nu)} \tag{7}$$

determining the relation $\omega(\beta_0)$.

4 NUMERICAL RESULTS

For the numerical evaluation we take the same dimensions as in [1] (all in mm)

$$a = 0.3\ ,\ b = 0.9\ ,\ w = 1.8\ ,\ d = 1.6\ ,\ g = 0.633\ ,\ t = 0.2$$

and a phase advance per cell equal $2\pi/3$.

For the acceleration mode we find a frequency $f = 122$ GHz, which aggrees very good with the MAFIA-result.

Furthermore the longitudinal shunt impedance divided by the Q-value

$$\frac{R}{Q} = \frac{Z_0}{k(g+t)}\frac{\left|\int_0^{g+t} E_z\,\mathrm{e}^{\mathrm{j}kz}\,\mathrm{d}z\right|^2}{\overline{W}/\varepsilon_0} \tag{8}$$

where

$$\frac{\overline{W}}{\varepsilon_0} = \frac{1}{4}\int\limits_V \left\{\vec{E}\cdot\vec{E}^* + Z_0^2\vec{H}\cdot\vec{H}^*\right\} \mathrm{d}V$$

was computed and the resulting value was

$$R/Q = 142\,\mathrm{k}\Omega/\mathrm{m}$$

which differs not much from the value given in [1].

Fig.3+4 show the dispersion relation of the first accelerating and deflecting mode and Fig.5+6 the corresponding electric field in the plane $x = 0$ for $2\pi/3$ phase advance per cell.

To illustrate the quality of field continuity Fig.5 shows the relative error of the magnetic field in the matching plane $y = a$. Except for points in the neighbourhood of the edges the mean error was less then 10% if we take into account $m \times n = 14 \times 10 = 140$ TE_y- and TM_y-modes in the cavity region. For the electric field the quality was somewhat better.

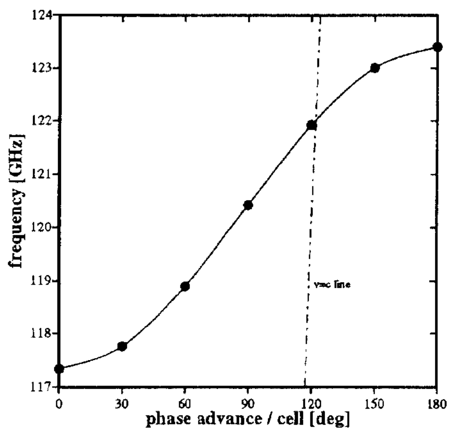

Figure 3: dispersion relation for the first accelerating mode

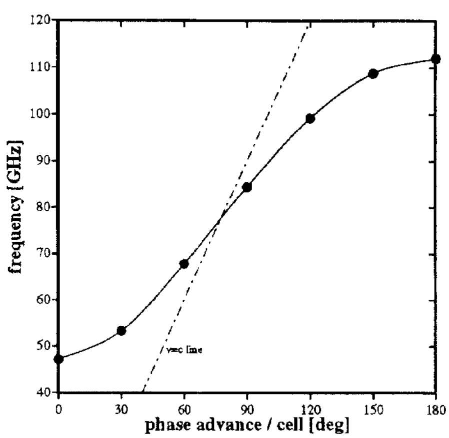

Figure 4: dispersion relation for the first deflecting mode

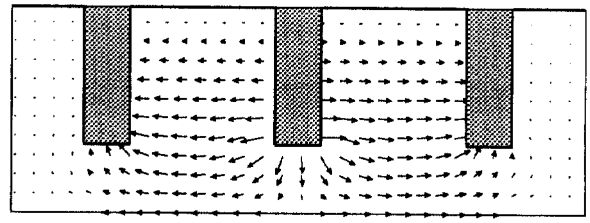

Figure 5: electric field of 1st accelerating mode (122 GHz)

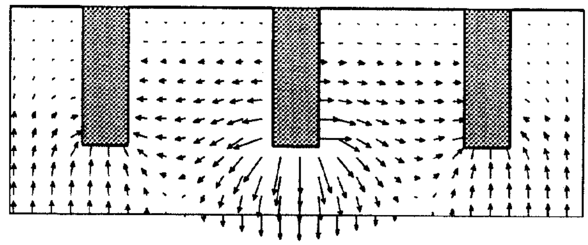

Figure 6: electric field of 1st deflecting mode (99.2 GHz)

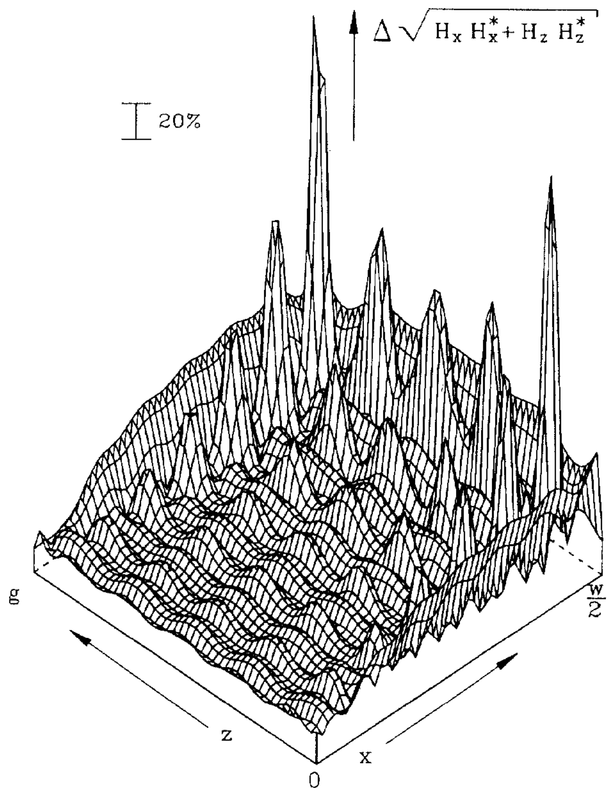

Figure 7: magnetic field error in the matching plane

5 REFERENCES

[1] H. Henke, Y.W. Kang and R. Kustom, "A mm-wave RF structure for relativistic electron acceleration", APS Note MMW-1, 1992